Magnetic phase transitions in the triangular antiferromagnetic system $CsMn(Br_xI_{1-x})_3$

1998 J. Phys.: Condens. Matter 10 7209

(http://iopscience.iop.org/0953-8984/10/32/012)

J. Phys.: Condens. Matter **10** (1998) 7209–7218. Printed in the UK PII: S0953-8984(98)93841-3

Magnetic phase transitions in the triangular antiferromagnetic system $CsMn(Br_xI_{1-x})_3$

T Ono, H Tanaka, T Kato and K Iio

Department of Physics, Faculty of Science, Tokyo Institute of Technology, Oh-okayama, Meguro-ku, Tokyo 152-8551, Japan

Received 1 May 1998

Abstract. $CsMnBr_3$ and $CsMnI_3$ are known to be triangular antiferromagnets with planar and axial magnetic anisotropy, respectively. Magnetic susceptibility and torque measurements have been carried out to investigate the relationship between the magnetic anisotropy and phase transition in the mixed triangular antiferromagnetic system, $CsMn(Br_xI_{1-x})_3$. The phase diagram for the Néel temperature T_N versus the bromine concentration x is obtained. With increasing x, the intermediate ferrimagnetic phase becomes narrower and it vanishes at $x_c = 0.19$, where the magnetic anisotropy generally vanishes.

1. Introduction

A number of hexagonal ABX_3 antiferromagnets with a crystal structure of $CsNiCl_3$ type have been studied in view of their phase transitions, magnetic excitations and critical phenomena for the last two decades. The crystal structure consists of BX_3 chains parallel to the c-axis, separated by monovalent A^+ ions. The magnetic B^{2+} ions form a triangular lattice in the basal plane.

The magnetic interactions in the ABX_3 antiferromagnets are usually represented by

$$\mathcal{H} = 2J_0 \sum_{\langle i,j \rangle}^{\text{chain}} \boldsymbol{S}_i \cdot \boldsymbol{S}_j + 2J_1 \sum_{\langle \ell,m \rangle}^{\text{plane}} \boldsymbol{S}_\ell \cdot \boldsymbol{S}_m + 2\,\Delta J \sum_{\langle i,j \rangle} S_i^z S_j^z + D \sum_i (S_i^z)^2 \tag{1}$$

where the first and second terms are the exchange interactions along the chain and in the basal plane, respectively. The third and last terms denote the pseudodipolar interaction and the single-ion anisotropy, respectively. Since J_0 is significantly larger than J_1 ($J_0/J_1 > 10^2$), with some exceptions, the ABX_3 antiferromagnets behave as one-dimensional spin systems at high temperatures. With decreasing temperature, the interchain spin correlation grows, with the result that three-dimensional ordering occurs. Since the J_1-interaction is antiferromagnetic, they are described as stacked triangular antiferromagnets (TAF) in the vicinity of and below the ordering temperature. Thus the spin frustration plays an important role in the phase transitions. Various kinds of successive phase transitions and novel critical behaviour have been observed in recent studies [1–8].

$CsMnBr_3$ and $CsMnI_3$ are typical examples of the stacked TAF with planar and axial anisotropy respectively. Their lattice and magnetic parameters are summarized in table 1. The origin of the anisotropy for both compounds is mainly the pseudodipolar interaction, which is shown in section 3.

0953-8984/98/327209+10$19.50

Table 1. Lattice and magnetic parameters of $CsMnBr_3$ and $CsMnI_3$. The values of ΔJ are estimated from the anisotropy energies given in references [9] and [10].

	$CsMnBr_3$	Reference	$CsMnI_3$	Reference
J_0/k_B	10.3 K	[11]	9.5 K	[12]
J_1/k_B	0.020 K	[11]	0.042 K	[12]
$\Delta J/k_B$	−0.070 K	[9]	0.025 K	[10]
T_N	8.37 K	[8]	$T_{N1} = 8.2$ K $T_{N2} = 11.2$ K	[13, 14]
a (at r.t.)	7.61 Å	[15]	8.20 Å	[16, 17]
c (at r.t.)	6.52 Å	[15]	6.96 Å	[16, 17]

$CsMnBr_3$ undergoes a phase transition at $T_N = 8.3$ K. In the ordered phase, the spins lie in the basal plane and form a 120° structure. $CsMnI_3$ has two phase transitions, at $T_{N1} = 11.2$ K and $T_{N2} = 8.2$ K. In the intermediate phase, the c-axis component of the spin is ordered, with ferrimagnetic structure in the basal plane. In the low-temperature phase, the perpendicular component of the spin is ordered, such that the spins form a triangular structure in the plane including the c-axis, i.e., one-third of the spins are parallel to the

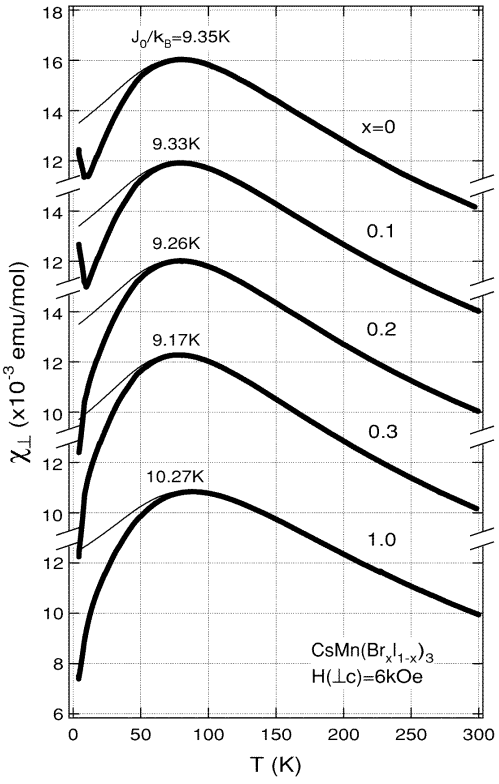

Figure 1. The temperature dependences of the perpendicular susceptibilities $\chi_\perp$ for the $CsMn(Br_xI_{1-x})_3$ system measured at $H = 6$ kOe. The thick lines show experimental results and the thin solid lines represent fits of Fisher's theory to our data for $T > 90$ K.

c-axis and the rest of the spins are canted away from the *c*-axis.

As observed for $CsMnBr_3$ and $CsMnI_3$, the phase transition and critical behaviour of the TAF depend on the anisotropy. Therefore, it is worth studying how the phase transition changes with the anisotropy. In this paper, we treat the magnetic anisotropy and the phase transition in the mixed system $CsMn(Br_xI_{1-x})_3$. The magnitude and the sign of the anisotropy are systematically controlled by varying the bromine concentration x. Since the present system contains only Mn^{2+} ions as the magnetic ions, the spin states are expected to be homogeneous. We measured the susceptibility and torque to investigate the anisotropy and phase transition in $CsMn(Br_xI_{1-x})_3$.

This paper is organized as follows. In section 2, experimental procedures are described. Experimental results and a discussion are given in section 3. The final section is devoted to the conclusions.

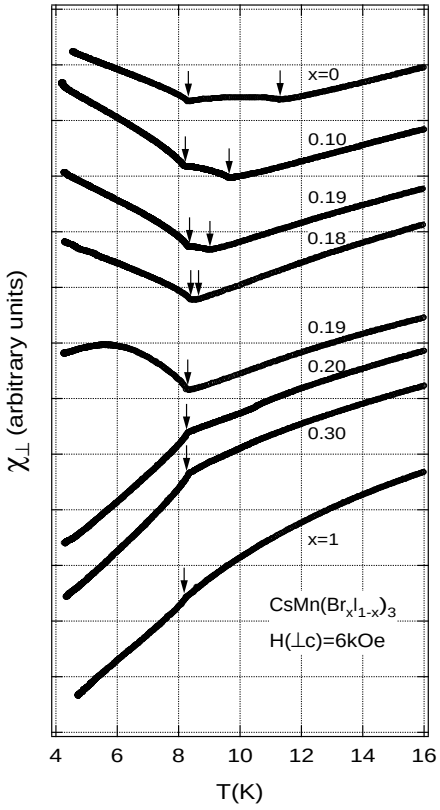

Figure 2. The temperature dependence of the perpendicular susceptibility $\chi_\perp$ for various values of x in the phase transition region. The arrows indicate phase transition points.

2. Experimental procedures

The single crystals of $CsMnBr_3$ and $CsMnI_3$ were grown by the vertical Bridgman method from a melt of equimolar mixtures of CsX and MnX_2 (X = Br and I) sealed in evacuated quartz tubes. The temperature at the centre of the furnace was set at 650 °C, and the

lowering rate was 3 mm h^{-1}. The source materials used were CsI and MnI_2 of 99.9% purity and $MnBr_2{\cdot}4H_2O$ of 99% purity (Soekawa Chemicals), and CsBr of 99.9% purity (Wako Pure Chemical Industries). To get manganese bromide, $MnBr_2{\cdot}4H_2O$ was dehydrated at around 120 °C in vacuum for three days. CsI, $MnBr_2$ and MnI_2 are very hygroscopic, so we treated them in a glove box filled with dry nitrogen. After weighing, the materials were packed into the quartz tubes and dehydrated in vacuum near 150 °C for three days, again.

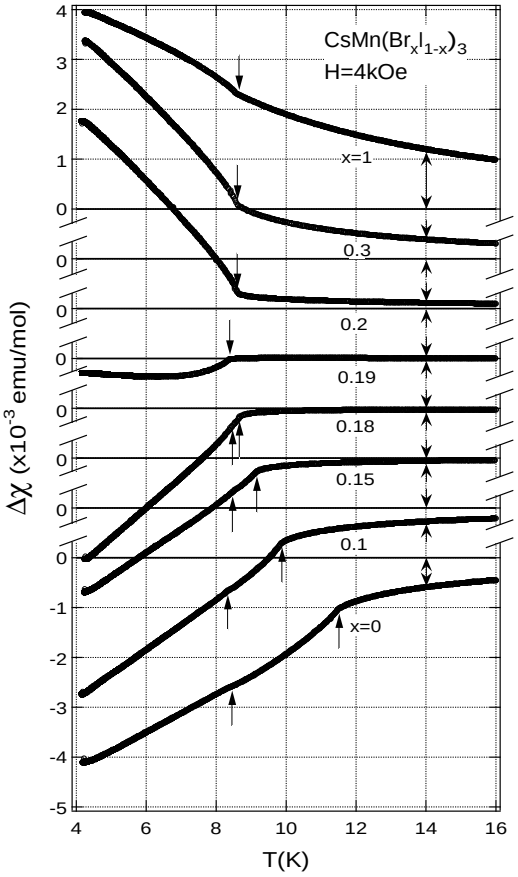

Figure 3. The temperature dependence of $\Delta\chi$ defined by $\Delta\chi = \chi_{\parallel} - \chi_{\perp}$ for the system $CsMn(Br_xI_{1-x})_3$ in the phase transition region measured at $H = 4$ kOe. Transition points are indicated by arrows.

Mixing single crystals of $CsMnBr_3$ and $CsMnI_3$ in the ratio of $x{:}1-x$, we prepared $CsMn(Br_xI_{1-x})_3$ by the Bridgman method. Single crystals of size 1–5 cm^3 were obtained. Each sample looks homogeneous, so the gradients of the bromine concentration are expected to be very small. The crystals are easily cleaved along the (1, 0, 0) plane. The samples were cut into pieces weighing 100–150 mg and coated with Apiezon-N grease.

The susceptibility was measured by the Faraday method using a Cahn 2000 electrobalance and an electromagnet. Accuracies of 5% in the absolute value and 1% in the relative value were obtained for the temperature variation. To measure the perpendicular susceptibility $\chi_{\perp}$ accurately, we defined the c-axis to be vertical so that the external field

was always perpendicular to it. Since the value of $\chi_{\parallel} - \chi_{\perp}$ is obtained by the torque measurement, we did not measure the susceptibility $\chi_{\parallel}$ which is parallel to the c-axis.

The torque meter used (Yasunami YMT-H1) is an electric current-to-torque transducer-type meter constructed for measuring torques as small as 10^{-4}–10^{-3} dyn cm. We measured the current which generates countertorque to keep the orientation of the sample unchanged. The accuracy is almost the same as that of the magnetometer. The sample was set such that the external field always lies in the (1, 1, 0) plane including the c-axis. The electromagnet was rotated at the rate of 1.5° s^{-1} for the measurements of the torque curves. The temperatures of the samples were measured with a Au–Fe thermocouple. The bromide concentration x was analysed by emission spectrochemical analysis after the measurements.

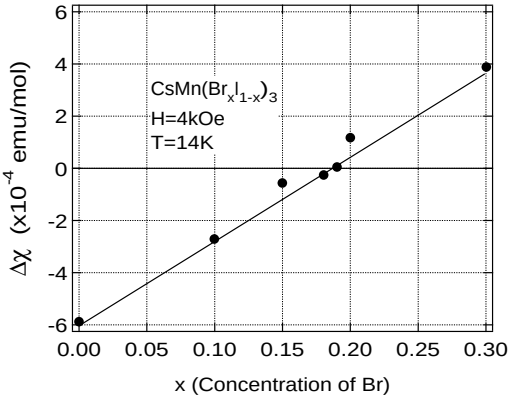

Figure 4. The differential susceptibility $\Delta\chi$ as a function of the bromine concentration x at $T = 14$ K. The solid line is a guide to the eye.

3. Results and discussion

3.1. Magnetic susceptibility

Figure 1 shows the temperature dependence of the susceptibility $\chi_{\perp}$ perpendicular to the c-axis for various bromine concentrations x. The applied magnetic field is 6 kOe. All of the susceptibility curves have the broad maxima at around 80 K, which is characteristic of one-dimensional Heisenberg antiferromagnets. In order to check the intrachain exchange interaction J_0, the susceptibility data above 90 K were fitted to Fisher's theory [18] for the classical Heisenberg linear chain. His result is expressed as

$$\chi(T) = \frac{4N_{\mathrm{A}}g^2\mu_{\mathrm{B}}^2 S(S+1)}{12k_{\mathrm{B}}T}\frac{1+u(K)}{1-u(K)} \tag{2}$$

with

$$u(K) = \coth K - \frac{1}{K}$$

and

$$K = \frac{1}{2}\frac{J_0}{k_{\mathrm{B}}T}.$$

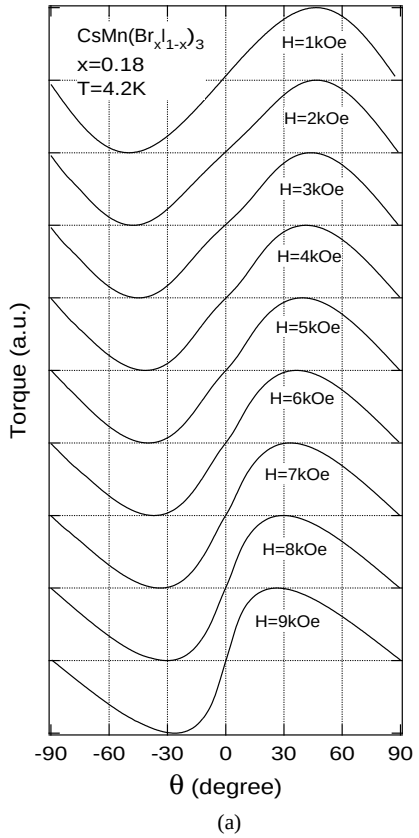

(a)

Figure 5. Torque curves at 4.2 K for (a) $x = 0.18$, (b) $x = 0.19$ and (c) $x = 0.20$.

Since the spin value of the present system is $S = 5/2$, equation (2) gives a good approximation to the high-temperature susceptibilities. The values of J_0 obtained from the fitting are shown in figure 1. For $x \leqslant 0.3$, the value of J_0 slightly decreases with increasing x.

Figure 2 shows the susceptibilities $\chi_\perp$ at low temperatures. Phase transitions are clearly seen at the positions indicated by arrows. Sharp anomalies due to the phase transitions are indicative of the good homogeneity of the samples. For the samples with $x = 0$, 0.1, 0.15 and 0.18, two phase transitions are observed. The susceptibility decreases monotonically with increasing temperature, has bend anomalies at T_{N2} and T_{N1} and then increases in the paramagnetic phase. This behaviour is typical of antiferromagnetically stacked TAFs for the weak-axial-anisotropy case [19, 20]. On the other hand, a single phase transition is observed at $T_N \approx 8.3$ K for the samples with $x = 0.2$, 0.3 and 1.0. The susceptibility increases monotonically and changes its gradient at the Néel temperature. This behaviour is typical of the planar-anisotropy case [21].

3.2. Magnetic torque

The magnetic torque $L(\theta)$ is given by $L(\theta) = -\partial F/\partial\theta$, where F is the free energy of the system and θ is the angle between the external field $\boldsymbol{H}$ and the c-axis. In the paramagnetic

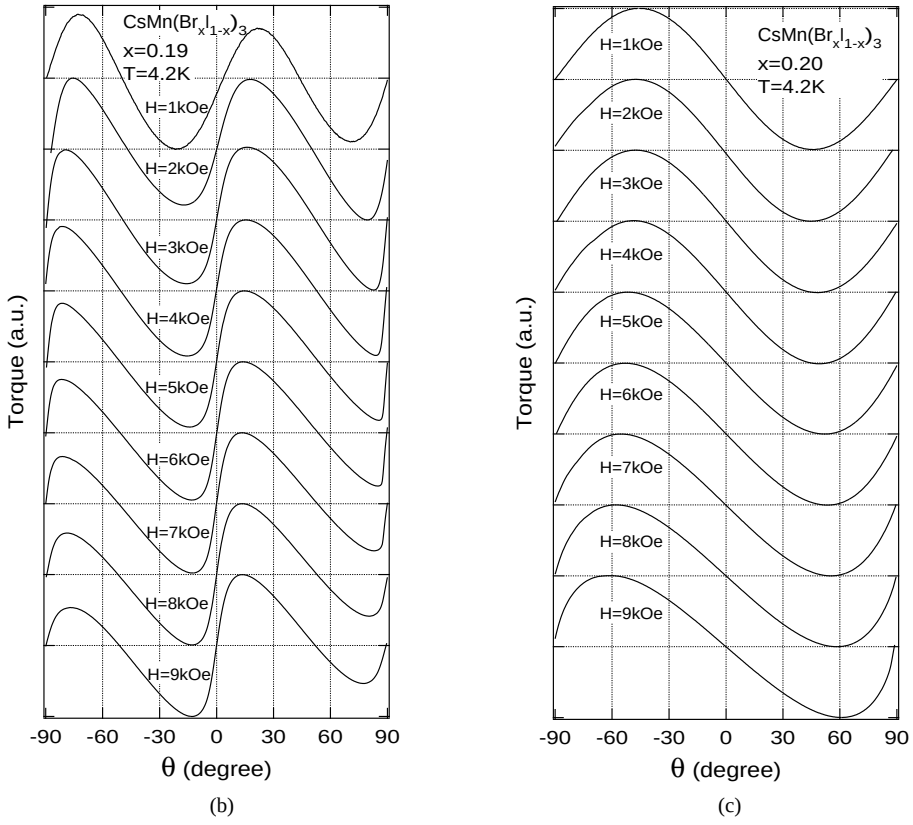

Figure 5. (Continued)

phase, $L(\theta)$ is expressed as

$$L(\theta) = -\frac{\partial F}{\partial \theta} = -\frac{1}{2}(\chi_{\parallel} - \chi_{\perp})H^2 \sin(2\theta) \tag{3}$$

where $\chi_{\parallel}$ and $\chi_{\perp}$ are the susceptibilities for $\boldsymbol{H} \parallel \boldsymbol{c}$ and $\boldsymbol{H} \perp \boldsymbol{c}$, respectively. Thus, we can obtain $\Delta\chi = \chi_{\parallel} - \chi_{\perp}$ through the torque measurement.

Nagata *et al* [22] demonstrated that for the one-dimensional antiferromagnet with the isotropic g-factor, $\Delta\chi$ does not change its sign over the entire temperature range when the anisotropy is due to the pseudodipolar interaction, while for the single-ion anisotropy, $\Delta\chi$ changes its sign at

$$T = J_0 S(S+1)/k_B.$$

We confirmed by ESR measurements that the g-factor in $CsMnBr_3$ and $CsMnI_3$ is almost equal to 2.00 irrespective of the magnetic field direction. We measured the torque on both the compounds up to room temperature and observed that $\Delta\chi$ does not change its sign. This shows that the origin of the magnetic anisotropy in the present systems is the pseudodipolar interaction, and is not the single-ion anisotropy.

Figure 3 shows the temperature dependence of $\Delta\chi$ defined by

$$\Delta\chi = -2L(\theta = 45^{\circ})/H^2.$$

When the torque is proportional to $H^2 \sin 2\theta$ in the ordered state, $\Delta\chi$ is equal to $\chi_{\parallel} - \chi_{\perp}$. Phase transitions are observed at the same temperatures as those detected by the susceptibility measurements. For $x < 0.19$, the lower-temperature phase transition (at T_{N2}) is less clear than that at the higher temperature (T_{N1}).

Figure 4 shows $\Delta\chi$ at 14 K. We see that the value of $\Delta\chi$ increases linearly in x, and it becomes zero at $x_c = 0.19$. Since $\Delta\chi$ is proportional to the magnitude of the anisotropy, this result indicates that the pseudodipolar interaction ΔJ generally varies as $\Delta J \propto (x_c - x)$, i.e., the anisotropy changes from axial type to planar at $x = x_c$.

In the antiferromagnetically stacked TAF, the 120° structure in the basal plane gives $\chi_{\parallel} > \chi_{\perp}$, while the triangular structure in the plane including the c-axis gives $\chi_{\parallel} < \chi_{\perp}$. Thus, it is concluded that the anisotropy is of axial type for $x < x_c = 0.19$, and of planar type for $x > x_c$, and that the ground-state spin structures for $x < x_c$ and $x > x_c$ are the same as those of $CsMnI_3$ and $CsMnBr_3$, respectively.

Figure 5 shows the torque curves at 4.2 K for $x = 0.18$, 0.19 and 0.20. The torque at low fields for $x = 0.18$ and 0.20 is roughly described by equation (3). On increasing the external field, the peaks shift towards the $\theta = 0$ for $x = 0.18$ and towards $\theta = \pm 90°$ for $x = 0.20$. This behaviour is interpreted as resulting from the fact that the plane of the triangular spin structure (the spin plane) moves slightly so as to become perpendicular to the external field. The anomaly near $\theta = 0°$ for $x = 0.18$ is attributed to the 'single-domain–multidomain' transition for the orientation of the spin plane, which is characteristic of the triangular spin structure including the c-axis [20]. The torque for $x_c = 0.19$ has a large component with a period of 90°. This implies that the anisotropy vanishes at $x = x_c$, and that the spin structure is mainly affected by the external field.

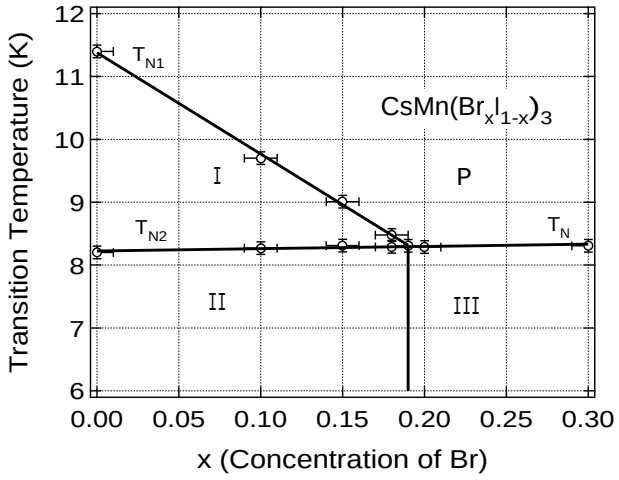

Figure 6. The phase diagram for the transition temperature versus the bromine concentration x.

3.3. The phase diagram

Figure 6 shows the phase diagram of the transition temperatures versus bromine concentration x obtained from the susceptibility and torque measurements. The experimental results are plotted as open circles with error bars. In this figure, P denotes the paramagnetic phase. The phase labelled III is the phase of the 120° structure in the c-plane. For $x < x_c$,

the intermediate (IM) phase and the low-temperature (LT) phase are labelled I and II, respectively. The magnetic structures in phases I and II are the two-sublattice ferrimagnetic structure and the triangular structure in the plane including the *c*-axis, respectively. As seen from figure 6, the intermediate phase I becomes narrower with increasing *x*, and vanishes at $x_c = 0.19$. The I–II and P–III phase boundaries are almost constant at 8.3 K. The boundary between phases II and III may be parallel to the temperature axis, because no phase transition was observed below $T = 8.3$ K for $x = 0.18$, 0.19 and 0.20.

Miyashita and Kawamura studied the phase transition within the anisotropic Heisenberg model on the triangular lattice by means of the Monte Carlo method [23]. They showed that the temperature range of the IM phase decreases on decreasing the magnitude of the axial anisotropy, and that the P–IM and IM–LT phase boundaries meet tangentially at the isotropic limit. In the present system, we could not observe such a tangential confluence of the two phase boundaries within the experimental resolution.

The phase transition and the critical behaviour of the TAF differ from those of unfrustrated spin systems due to the new degree of freedom, namely the chirality [24]. Kawamura pointed out that the stacked XY- and Heisenberg TAFs belong to the chiral universality classes characterized by new critical exponents [4], which are different from those of unfrustrated spin systems, i.e., $\alpha = 0.34$, $\beta = 0.25$, $\gamma = 1.13$ and $\nu = 0.54$ for the XY-spin and $\alpha = 0.24$, $\beta = 0.30$, $\gamma = 1.17$ and $\nu = 0.59$ for the Heisenberg spin. Kawamura's prediction for the XY-TAF was confirmed by neutron scattering and specific heat measurements on $CsMnBr_3$ [5–8]. For the critical behaviour of the Heisenberg TAF, however, no systematic study has been performed, because there is no suitable compound available. Our system, CsMn(Br_xI_{1-x})$_3$ with $x_c = 0.19$ is a candidate which belongs to the chiral Heisenberg universality class. Therefore, it is of great interest to investigate the critical behaviour of the present system.

4. Conclusion

Magnetic phase transitions in the triangular antiferromagnetic system CsMn(Br_xI_{1-x})$_3$ have been studied by susceptibility and torque measurements. The phase diagram for the ordering temperature and bromine concentration *x* was obtained and this is shown as figure 6. With increasing *x*, the higher transition temperature decreases linearly with *x*, and the intermediate phase vanishes at $x_c = 0.19$. The magnetic anisotropy changes from axial (easy-axis) type to planar (easy-plane) type at $x = x_c$, where the system becomes isotropic.

References

[1] Goto T, Inami T and Ajiro Y 1990 *J. Phys. Soc. Japan* **59** 2328
[2] Katori H A, Goto T and Ajiro Y 1992 *J. Phys. Soc. Japan* **62** 743
[3] Kawamura H, Caillé A and Plumer M L 1989 *Phys. Rev.* B **41** 4416
[4] Kawamura H 1992 *J. Phys. Soc. Japan* **61** 1299
[5] Ajiro Y, Nakashima T, Unno Y, Kadowaki H, Mekata M and Achiwa N 1988 *J. Phys. Soc. Japan* **57** 2648
[6] Mason T E, Gaulin B D and Collins M F 1989 *Phys. Rev.* B **39** 586
[7] Kadowaki H, Shapiro S M, Inami T and Ajiro Y 1988 *J. Phys. Soc. Japan* **57** 2640
[8] Deutschmann R, von Löhneysen H, Wosnitza J, Kremer R K and Visser D 1992 *Europhys. Lett.* **17** 637
[9] Falk U, Furrer A, Güdel H U and Kjems J K 1987 *Phys. Rev.* B **35** 4888
[10] Inami T, Kakurai K, Tanaka H, Enderle M and Steiner M 1994 *J. Phys. Soc. Japan* **63** 1530
[11] Gaulin B D, Mason T E and Collins M F 1989 *Phys. Rev. Lett.* **62** 1380
[12] Zandbergen 1980 *J. Solid State Chem.* **35** 367
[13] Iio K, Hotta H, Sano M, Masuda H, Tanaka H and Nagata K 1988 *J. Phys. Soc. Japan* **57** 50
[14] Harrison A, Collins M F, Abu-Dayyeh J and Stager C V 1991 *Phys. Rev.* B **43** 679

[15] Goodyear J and Kennedy D J 1972 *Acta Crystallogr.* B **28** 1640
[16] McPherson G L, Sindel L J, Quals H F, Frederich C B and Doumit C J 1975 *Inorg. Chem.* **14** 1831
[17] Sanchez J P, Friedt J M, Djermouni B and Jehanno G 1979 *J. Phys. Chem. Solids* **40** 585
[18] Fisher M E 1969 *Am. J. Phys.* **32** 343
[19] Brener R, Ehrenfreund E and Shechter H 1977 *J. Phys. Chem. Solids* **38** 1023
[20] Tanaka H, Hasegawa T and Nagata K 1993 *J. Phys. Soc. Japan* **62** 4053
[21] Tanaka H, Nakano H and Matsuo S 1994 *J. Phys. Soc. Japan* **63** 3169
[22] Nagata K, Tazuke Y and Tsushima K 1972 *J. Phys. Soc. Japan* **32** 1486
[23] Miyashita S and Kawamura H 1985 *J. Phys. Soc. Japan* **53** 3385
[24] Miyashita S and Shiba H 1984 *J. Phys. Soc. Japan* **53** 1145